PROCEEDINGS, 43rd Workshop on Geothermal Reservoir Engineering
Stanford University, Stanford, California, February 12-14, 2018
SGP-TR-213

Analysis of Magma Injections beneath Mutnovsky Volcano (Kamchatka)

Alexey V. Kiryukhin[1], Andrey Y. Polyakov[1], Petr A. Kiryukhin[2]

[1]- Institute of Volcanology and Seismology FEB RAS, Piip-9, Petropavlovsk Kamchatsky 683006 Russia

AVKiryukhin2@mail.ru

[2]- EPAM, Zastavskaya 22-2, Mega Park, Saint Petersburg 196084 Russia

Keywords: magma, injection, active, volcano, seismicity, CFRAC, Frac-Digger

ABSTRACT

For this study we used Frac-Digger program to identify plane-oriented MEQ clusters beneath Mutnovsky volcano. Magma injection events (dykes and sills) are associated with plane-oriented MEQ clusters (2009-2017), most of them are located in NE sector of the volcano (2 x 10 km^2) at the elevations from -2.0 to -4.0 km and indicate RF stress conditions beneath Mutnovsky volcano. CFRAC (M. McCluer, R. Horne, 2014) modeling of magma injection into the fracture, characterized by the conditions of Mutnovsky volcano basement (reverse fault, dip angle 30°, sizes 4 x 4 km^2, depth – 3 km below sea level) was performed. CFRAC modeling shows that magma injection rate of 2000 kg/s during 1 day may cause: fracture shear displacement up to 10 m and triggering up to several hundreds of earthquakes with magnitudes up to 6.1. Modeling results matches with MEQ magnitudes observed.

1. INTRODUCTION

This work treats the emplacement of magma in a fractured medium beneath active volcanoes by analogy to fluid injection into wells with subsequent hydraulic fracturing and fracture generation in host formations. This approach is also motivated by the observations reported by Sigmundsson et al. (2015), who described the injection of magma from the magma chamber beneath the Barparbunga central-type volcano, Iceland, which occurred in August 2014 and was accompanied by a dyke that propagated at the distance of 50 km. This dyke system with the volume of 0.6 km^3 was created during 22 days, it was segmented into 11 plane-oriented earthquake cluster zones (the number of earthquakes in each cluster is from 57 to 1181 with magnitudes of some earthquakes exceeding 5).

For this study, we used plane-oriented earthquake clusters (retrieved from the Kamchatka Branch Federal Research Center of the United Geophysical Survey of Russia's Academy of Sciences (KB FRC UGS RAS) Geophysical Survey catalogs (01.2009-02.2017) to track the dykes injected beneath and around the Mutnovsky volcano by using the method (the Frac-Digger program) described and verified in Kiryukhin et al., 2016, and Kiryukhin et al., 2017. Five seismic stations can record seismicity in the Mutnovsky-Gorely volcanic cluster (Fig. 1). A total of 1336 earthquakes were recorded by the KB FRC UGS RAS in the edifices and basement of the Mutnovsky and Gorely volcanoes between January 2009 and February 2017. For our treatment of this data we used the method outlined above, which yielded 973 earthquakes that make up 64 plane-oriented clusters between November 2013 and October 2016 as associated with the Mutnovsky volcano.

Cluster identification was carried out by using our Frac-Digger program (RU #Reg. 2016616880). The following criteria were used to include a new event in the cluster: (1) time difference (δt = 1 month); (2) distance difference in the horizontal plane less than 6 km; (3) the requirement of nearly planar orientation (distance from the event to the fitting plane of less than 1000 m); and (4) the number of elements in the cluster is greater than 5. The equation of the fitting plane $z = ax + by + c$ was found by using the least-squares method. The result is in the geological parameters of dip angle, dip azimuth and fracture area (which is defined as the area of polygon including cluster event projections on a fitting plane).

2. MUTNOVSKY PLANE-ORIENTED CLUSTER PROPERTIES & GEOMECHANICAL CONDITIONS

2.1 Plane-oriented cluster properties

The analysis of seismic activity at the Mutnovsky volcano revealed the following geomechanical features (Figs. 1-2). 1. Most of the plane-oriented MEQ clusters (which were interpreted as a dykes) were injected below in the northeastern sector of the Mutnovsky volcano in the area of 2 km x 10 km; 2. Most of the dykes beneath the Mutnovsky volcano have a dip angle ranging from 20-40°; 3. Most of the dykes were injected at the depth ranging from -4.0 to -2.0 km abs and at strikes in NE-NNE (30-50°) direction; 4. Seismic events of magnitude M during dyke injection ranged from 1.0 to 2.8; 5. Average area of MEQ-filled polygons of plane-oriented clusters is 17.2 km^2.

Thus, dyke geometry indicated reverse fault (RF) geomechanic conditions (Zoback, 2007) in the vicinity of the Mutnovsky volcano ($S_{Hmax} > S_{hmin} > S_v$, S_{Hmax} striking to NE).

2.2 Geomechanical conditions

Seismological observations were used to constrain our conceptual model of hydromechanical processes that might have occurred at the depth beneath the volcano. We assumed a simplified model geometry consisting of a single preexisting fracture to host the dike, and performed our investigation using the CFRAC numerical modeling (McClure, 2013, 2014). Based on the focal mechanisms of seismicity, we assumed a reverse faulting stress regime beneath Mutnovsky Volcano (Fig. 3), such that the vertical stress, S_v, is the minimum principal stress, the maximum horizontal stress, S_{Hmax}, acts in North-West direction, and the minimum horizontal stress, S_{hmin}, acts in North-East direction. At the depth of z_0=4500 m (≈ -3000 masl) S_v may be estimated as $S_v=\int_0^{z0} \rho \cdot g \cdot dz$ = 113.3 MPa (according to Table 1 properties vs depth); $S_{Hmax}= P_f+(S_v- P_f)\cdot((\mu^2+1)^{0.5}+\mu)^2$=279.3 MPa (where P_f is fluid pressure assumed to be 35 MPa based on water levelling data extrapolation to -3000 masl, friction coefficient μ=0.6); S_{hmin} was assumed to be roughly equal $(S_v+S_{Hmax})/2$ = 196.3 MPa.

Table 1 Input data for Sv estimations: rock properties vs depth

Range of depth masl	Dry rock density, kg/m^3	Porosity	Saturation	Lithology
1000, 1500	2200	0.30	SG=1	Andesite-basalt lavas Q_{3-4}
400, 1000	2400	0.20	SG=1	Pliocene-quarternary lavas and tuffs N_2-Q_1
200, 400	2400	0.20	SG=0	Miocene rhyolite tuffs N_1al
-1900, 200	2500	0.08	SG=0	Miocene sandstones Pg_3-N_1
-3500, -1900	2700	0.03	SG=0	Dyke intrusions zone Q_{3-4}

Based on the above, the effective stress tensor below Mutnovsky at the depth of -3000 masl is defined in the principal stress coordinate system X, Y , Z (X – SE direction, Y – NW direction, Z – upward direction, see Fig.3) in the following way (see also Fig. 3):

$$Sg = \begin{pmatrix} SHmax - Pf & 0 & 0 \\ 0 & Shmin - Pf & 0 \\ 0 & 0 & Sv - Pf \end{pmatrix} \quad (1)$$

Where S_{Hmax}= 279.3 MPa, S_{hmin} = 196.3 MPa, S_v= 113.3 MPa and P_f =35 MPa, as defined above.

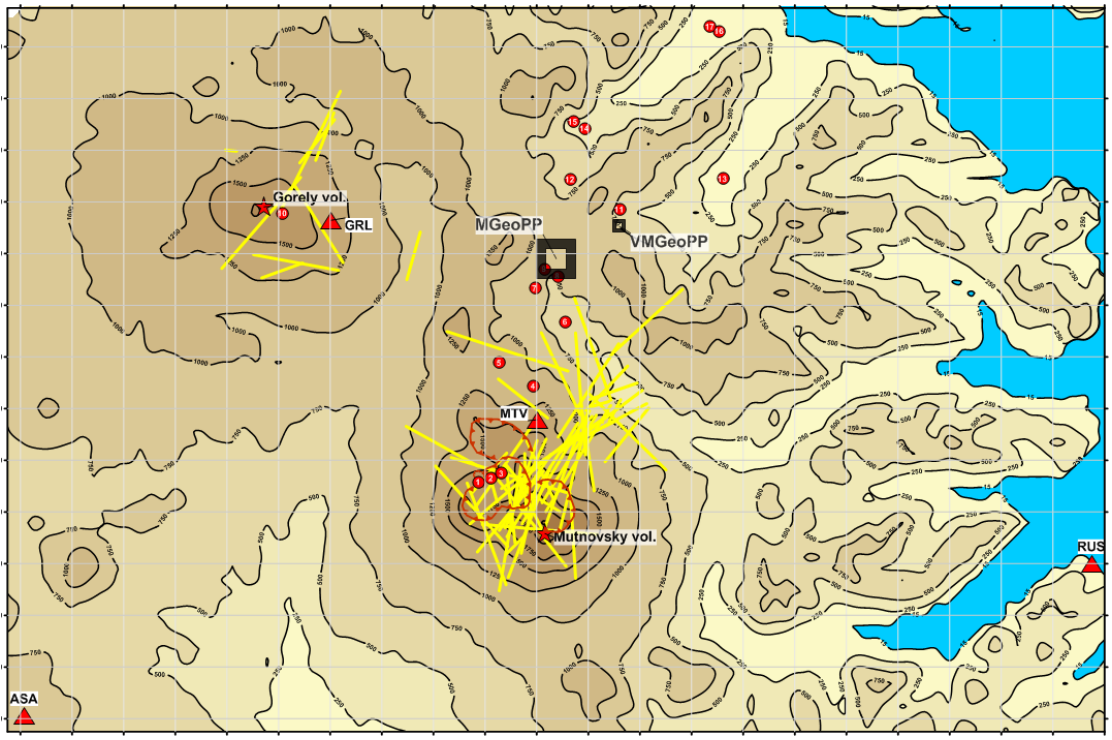

Figure 1: A schematic map of the Mutnovsky geothermal area: Circles with numbers are thermal occurrences. Triangles are the KB FRC UGS RAS seismic stations: MTV, GRL, ASA, RUS, PET. Yellow lines are traces of plane-oriented MEQ's clusters (interpreted as dyke traces) at the elevation -3000 masl. Isolines show the topographic surface, the ticks along the axes stand at intervals of 2 km. Note: this Figure does not show PET seismic station, which is 72 km NNE from Mutnovsky volcano summit.

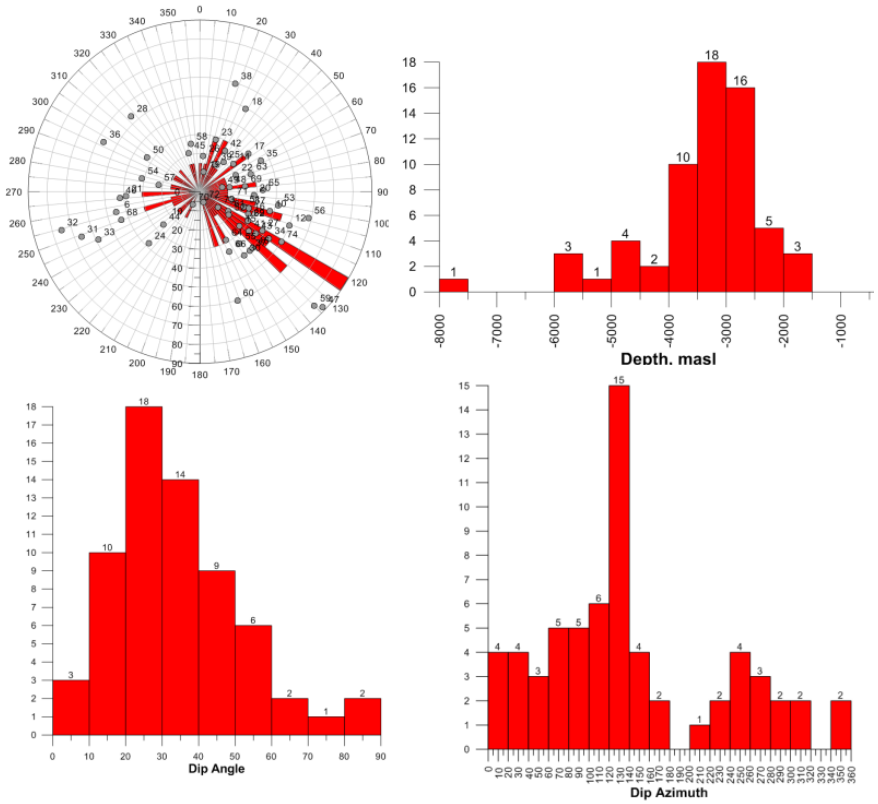

Figure 2: Dykes swarm stereogram (upper left) and hystograms (depth, dip angle and dip azimuth) below Mutnovsky volcano.

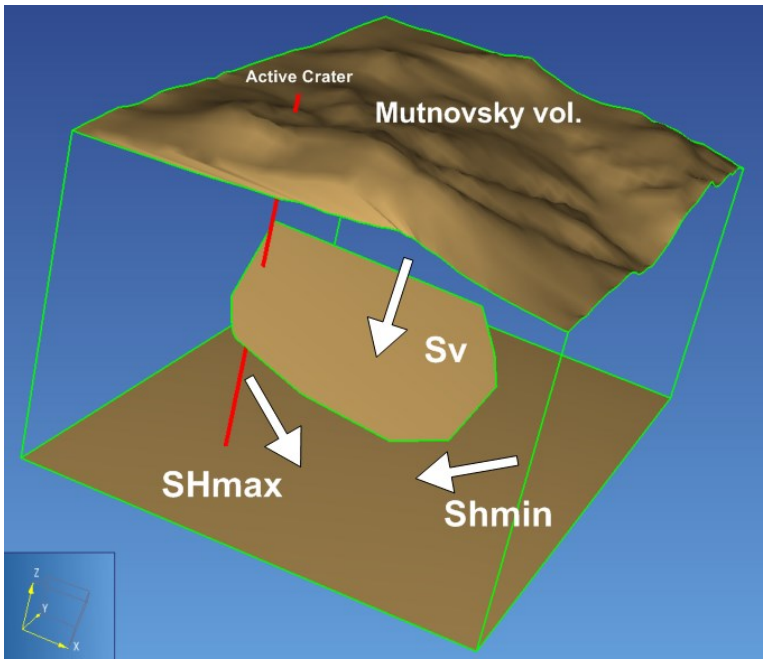

Figure 3 Conceptual model of dyke formation during magma injection beneath Mutnovsky volcano. S_v – vertical stress, S_{Hmax} – maximum horizontal stress, S_{hmin} – minimum horizontal stress.

3. CFRAC HYDROMECHANICAL MODELING

3.1 Model setup

The CFRAC model performs the solution of a coupled system of hydromechanical equations for flow and deformation in discrete fracture networks (McClure, 2014; McClure and Horne, 2013). When running 3D Simulations in CFRAC, you need to keep in mind, that: 1. CFRAC really deals with vertical fracs; 2. If you want to model an inclined frac, you have to rotate your XYZ coordinate system around Y axis to a new local coordinate system with Z2 axis parallel to frac plane (Y2 = Y); 3. Then you have to define effective stresses in a new coordinate system X2,Y2, Z2: S_{xx}, S_{yy}, S_{zz}, S_{xz} and Z2-trends of them (thus S_{xy} in terms of CFRAC is indeed S_{xz}). CFRAC code identifies the threshold value of shear displacement velocity to trigger/stop the earthquake as 5 mm/s and 2.5 mm/s, respectively (default values of meqstartvel and meqendvel parameters, McCluer, pers.com. 2017). At that moment the model element where this condition is achieved is interpreted as the initial point of earthquake rupture, which is closed when shear displacement velocities drop down to the above mentioned threshold value. The earthquake parameters identified in such a way with CFRAC (times, hypocenter coordinates, seismic moments and magnitudes, earthquake rupture areas) are kept in output files. Seismic moment M_0 is estimated in the relation to shear displacement case as: $M_0 = G \cdot \int slip\, dA$, where G – shear modulus, A – area of displacement. Then magnitude M_w is estimated as: $M_w = \lg(M_0)/1.5 - 6.06$ (where M_0 is expressed in N·m). In this work static/dynamic option (friction coefficient μ_{static}=0.6 when not sliding, it abruptly drops to $\mu_{dynamic}$=0.55 when it starts sliding) was used.

We considered a basic scenario of the dyke injection in the fracture with a dip angle of 30° and that was 4 km (dip direction) by 4 km (strike direction) centered at the depth of 4500 m (or -3000 masl) beneath Mutnovsky Volcano (the size and dip angle were determined with the Fig. 2). We assumed the following conditions: magma injection in the fracture took place within 1 day, magma injection rate was 2000 kg/s, and the maximum injection pressure was 200 MPa. Magma density was 2800 kg/m^3. We tested a range of magma viscosity between 2 Pa s (andesitic magma) and 2 Pa s (basaltic magma). The initial magma pressure was assigned 78.3 MPa, as fluid pressure was required for fracture activation, according to Mohr diagram (Fig. 4). Some additional scenarios were modeled too, see Table 2 listing model parameters.

Table 2 Model parameters and their values. Note: Stresses are in principal stress coordinate system at the depth of -3000 masl.

Parameter	Value	Unit
Sv	113.3	MPa
SHmax	279.3	MPa
Shmin	196.3	MPa
Shear modulus	15000	MPa
Poisson's ratio	0.25	
Stiffness constants	10	MPa
Magma viscosity	from 9e-5 to 2	Pa s
Magma density	2800	kg/m^3
Initial water pressure	35	MPa
Initial magma pressure	+78.3	MPa
Maximum injection pressure	200	MPa
Magma flowrate	2000	kg/s
Duration	1	day
Fracture dimensions	4 x 4 and 2 x 2	km

The effective stress tensor S_f in fracture coordinate plane (X2 – dip direction, Y2 – azimuth direction, Z2 - normal upward to fracture plane) was calculated (in units of MPa) with the known effective stress tensor in the principal stress coordinate system using the coordinate conversion matrix:

$$A = \begin{pmatrix} \cos(\beta)\cdot\cos(\alpha) & -\cos(\beta)\cdot\sin(\alpha) & -\sin(\beta) \\ \sin(\alpha) & \cos(\alpha) & 0 \\ \sin(\beta)\cdot\cos(\alpha) & -\sin(\beta)\cdot\sin(\alpha) & \cos(\beta) \end{pmatrix} \quad (2)$$

-where α is a strike azimuth (in case of principal stress coordinate system α=0), β is a dip angle (β=30°). Accordingly:

$$S_f = A \cdot S_g \cdot A^T \quad (3)$$

- where A^T is a transposed matrix of A.

Thus S_f is defined:

$$S_f = \begin{pmatrix} 202.8 & 0 & 71.9 \\ 0 & 161.3 & 0 \\ 71.9 & 0 & 119.8 \end{pmatrix} \qquad (4)$$

Then in terms of CFRAC: S_{xx}=119.8 MPa, S_{yy}=161.3 MPa, S_{zz}=202.8 MPa, S_{xy}= 71.9 MPa. Since there is no gravity included in CFRAC, then we have to assign effective stress trends in fracture coordinate system: $\frac{\partial Sxx}{\partial z}$ = 12.4 MPa/km, $\frac{\partial Syy}{\partial z}$ = 16.7 MPa/km, $\frac{\partial Szz}{\partial z}$ = 21.0 MPa/km, $\frac{\partial S_{xy}}{\partial z}$ = 7.4 MPa/km. These stress gradients were calculated numerically as based on stress tensor expression, using dZ derivates and water density for fluid pressure estimates. In case we assume magma as an effective stress managing fluid, then we have effective stress trends in fracture coordinate system: $\frac{\partial Sxx}{\partial z}$ = -1.3 MPa/km, $\frac{\partial Syy}{\partial z}$ = -1.0 MPa/km, $\frac{\partial Szz}{\partial z}$ = -1.7 MPa/km, $\frac{\partial S_{xy}}{\partial z}$ = -0.6 MPa/km.

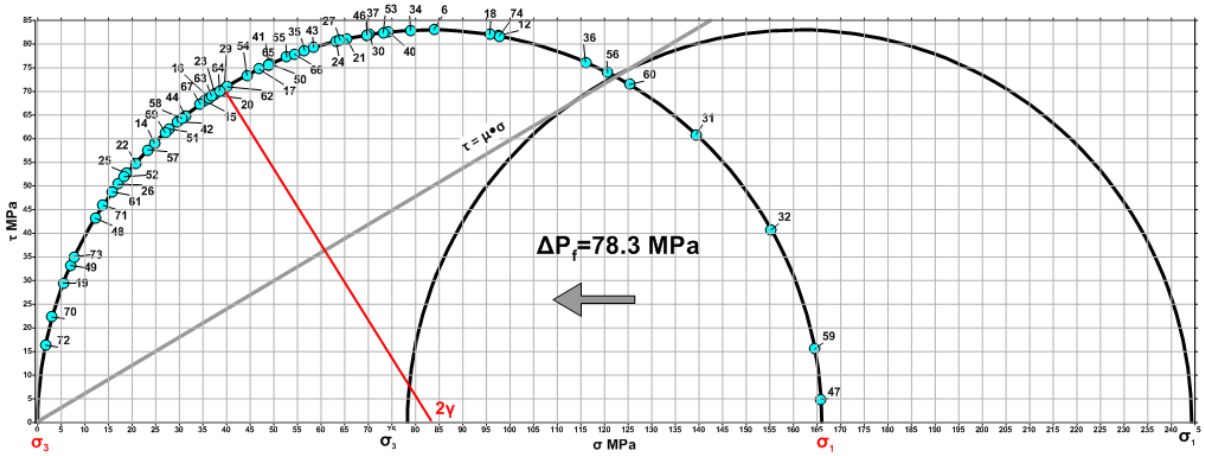

Figure 4 Mohr diagrams, which show effective stresses (σ_1=σ_{HMax}, σ_3=S_v) variations due to magma injection at the basement of Mutnovsky Volcano at the depth of 4500 m (≈ –3000 m abs.). The circle on the right covers the range of normal and shear stresses before the injection, the circle on the left is for the time after the injection, dots with numerals correspond to dipping angles of dikes and sills (plane-oriented earthquake clusters). A dot is positioned on a circle by measuring the angle 2γ with the apex at the center from the horizontal axis where $\gamma = 90^o$ - dip angle (β) of the plane-oriented cluster.

3.2 Modeling results

Modeling in the range of different magma viscosities, fracture sizes and two cases of the effective stress trends (using magma or water hydrostatics) was performed (total number of modeling scenarios was eight, Table 3). The following distributions of fracture properties one day after the injection started were obtained: fluid pressure and normal effective stress distributions, sliding vectors and fracture sliding velocity, fracture aperture distributions, MEQ's hypocenters, times and magnitudes.

Results of #1 scenario of CFRAC modeling (Table 3) is shown in Fig. 5 and 6. The re-opened part of the fracture is asymmetrically extended upward and is characterized by fluid pressure from 98 to 122 MPa (overpressure from 20 to 44 MPa), the effective normal stress was reduced to zero in this area, shear displacement during the injection triggers 339 of earthquakes at different times and different distances from the injection point with magnitudes up to 6.03 (Fig. 5). Fracture opening is up to 0.05 m (upper part) and up to 0.04 m (central part) (Fig. 6). The upper fracture wall slides up in relation to the lower fracture wall (reverse fault type). Up to 9.5 m of slip occurred in the central part of the fracture. MEQ's distributions (Fig. 5) seem to coincide with slip amplitude distributions (Fig.6), note also MEQ's tendency to set in the opening part of fracture (Fig. 5).

While in the case of water effective stress weighting the tendency of fracture upward opening was observed, in the case of magma effective stress weighting (Table 3, scenarios ## 2 & 3) the fracture central part is opening. Other modeling scenarios (## 4-8) listed in Table 3 show similar results to #1.

Table 3 Modeling scenarios.

##	effective stress trends	Viscosity Pa*s	Frac. size km x km	Magma rate kg/s
1	H_2O	2	4 x 4	2000
2	magma	2	4 x 4	2000
3	magma	2	2 x 2	2000
4	H_2O	2	2 x 2	2000
5	H_2O	2	4 x 4	200
6	H_2O	0.2	4 x 4	2000
7	H_2O	9e-5	4 x 4	2000
8	H_2O	9e-5	2 x 2	2000

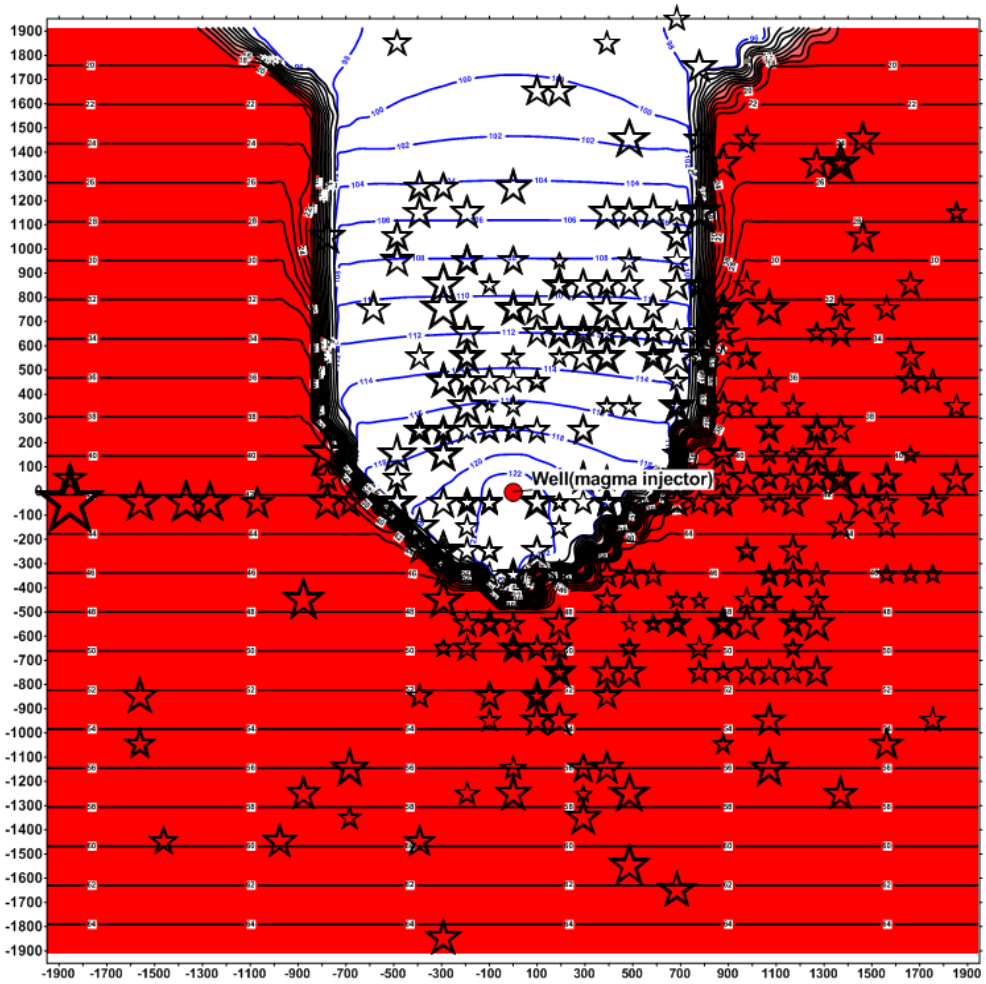

Figure 5 Magma pressure distribution in fracture plane (blue isolines, MPa), effective normal stress (black isolines, MPa) and earthquakes triggered by injection (stars, linear scaling to magnitude in the range from 0.99 to 6.03) one day after the magma injection started. CFRAC modeling scenario #1 (Table 3).

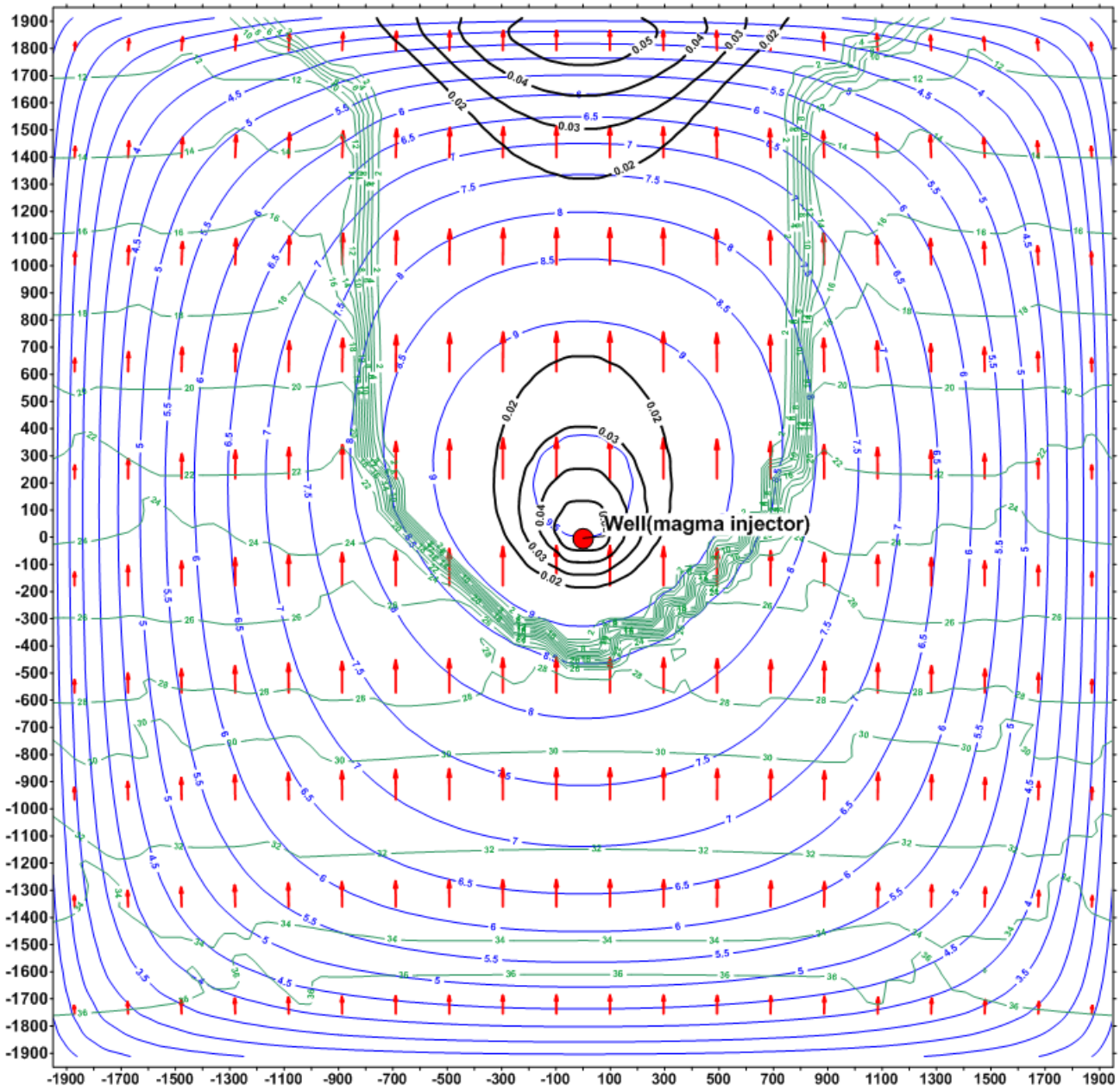

Figure 6 Fracture aperture (black isolines, m), sliding (blue isolines, m), shear stress (green isolines, MPa) and vectors of sliding (hanging block in relation to laying block) distributions. CFRAC modeling scenario #1 (Table 3).

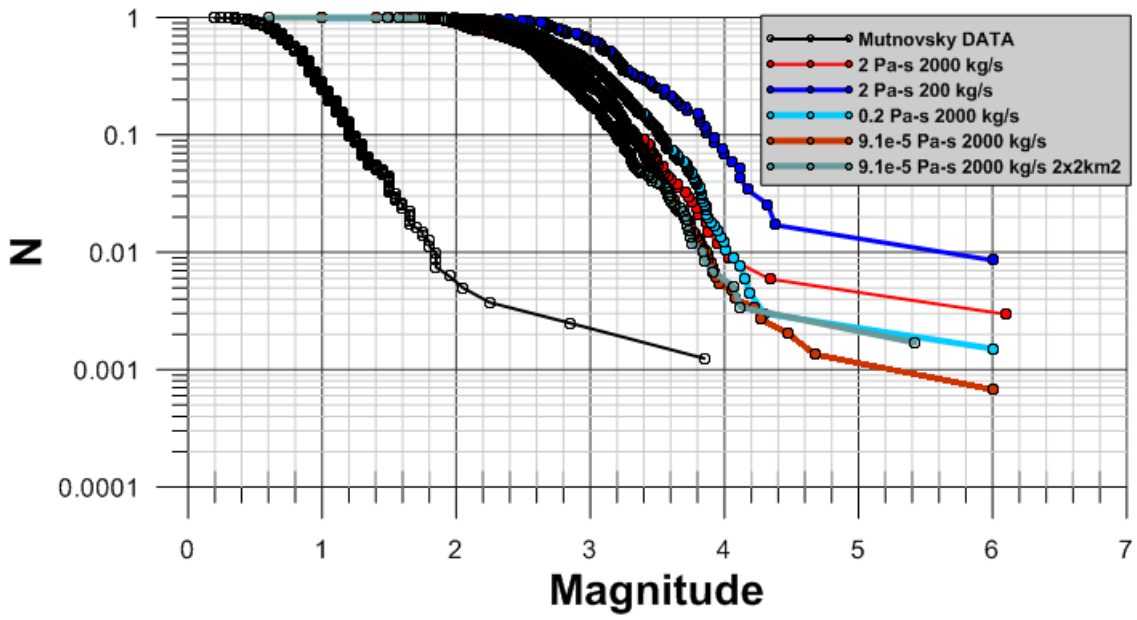

Figure 7 Gutenberg-Richter diagram of seismicity: earthquakes data beneath Mutnovsky volcano 01.2009-02.2017 and earthquakes generated in the hydrogeomechanical model (CFRAC) for magma injection in a 30°-dip pre-existing fracture (static/dynamic options) in the range of modeling scenarios with water effective stress trends were assumed (scenarios ##1, 5-8, Table 3).

4. DISCUSSION/CONCLUSIONS

CFRAC modeling of magma injection into the fracture, characterized by the conditions of Mutnovsky volcano basement (reverse fault, dip angle 30°, sizes from 2 x 2 km^2 to 4 x 4 km^2, depth – 3 km below sea level) was performed. Modeling shows that magma injection rate of 2000 kg/s during 1 day will cause: fracture opening with the aperture up to 0.05 m and shear displacement which trigger a few hundreds of earthquakes with magnitudes up to 6. Thus, it is feasible, that plane oriented clusters of earthquakes beneath active volcanoes may indicate magma-fracking or dyke formation processes.

Nevertheless, a different statistics of the observed earthquakes and modeling earthquakes was found (Fig. 7): (1) Two-order larger magnitudes of modeling MEQ's compare to the observed MEQ's; (2) A maximum number of the observed MEQ's in one cluster is 61, while a few hundreds of MEQ's within one injection events was found at modeling.

Generally, the largest earthquake in the model will be controlled by the largest fault size in the model. Having a pretty big fault in the model (4 x 4 km^2) means the upper limit is very high. Nevertheless, reducing the size of the fracture to 2 x 2 km^2 (#3, 4, 8, Table 3) doesn't help a lot (Fig. 7). Alternatively, we may consider increasing $\mu_{dynamic}$ to be closer to μ_{static}. The closer together, the less stress drop will occur in each event. However, we should note that won't reduce the overall amount of slip so that it is likely to affect the b-value, but not necessarily the total seisimic magnitude release. A third (heuristic) option would be to postprocess by making some assumption about the amount of slip that is seismic. We might suppose that not all slip is seismic, a certain percentage of slip occurs aseismically. CFRAC does not capture that because it uses homogeneous frictional properties. One may say that 99% of slip is aseismic (doesn't create MEQ). Then take 99% MEQ's out of the model, thus recalculating moment/magnitude statistics.

We also have to note a non-symmetric MEQ's hypocenter distributions (Fig.5), while geometrically symmetric input model was used. This may be explained that doing static/dynamic friction treatment does not provide a fully meshed converged exact solution to a well-defined PDE. This is due to the abrupt weakening of friction which is kind of numerically mesh dependent. This is in contrast to the rate/state friction. Not having an exact solution isn't ideal, but the results are still qualitatively reasonable.

Authors appreciate help and useful comments of Dr. M. McCluer. This work was supported by RSF grant # 16-17-10008.

REFERENCES

Kiryukhin A.V., Fedotov S.A., and Kiryukhin P.A.: A Geomechanical Interpretation of the Local Seismicity Related to Eruptions and Renewed Activity on Tolbachik, Koryakskii, and Avacha Volcanoes, Kamchatka, in 2008–2012, Journal of Volcanology and Seismology, 10(5), (2016), 275–291.

Kiryukhin A., Norbeck J. Analysis of Magma Injection Beneath an Active Volcano Using a Hydromechanical Numerical Model PROCEEDINGS, 42nd Workshop on Geothermal Reservoir Engineering Stanford University, Stanford, California, February 13-15, 2017, p.740-747.

Kiryukhin A. Analysis of Magma Injection Beneath an Active Volcano Using a Hydromechanical Numerical Model (CFRAC) // EAGE conference "Horizontal wells", Kazan. 2017. 4 p. DOI: 10.3997/2214-4609.201700475

Kiryukhin A., Lavrushin V., Kiryukhin P., Voronin P. Geofluid Systems of Koryaksky-Avachinsky Volcanoes (Kamchatka, Russia) // Geofluids, vol. 2017, Article ID 4279652. 21 pages. 2017. doi:10.1155/2017/4279652.

Kiryukhin A.V., Fedotov S.A., Kiryukhin P.A., Chernykh E.V. Magmatic plumbing systems of the Koryakskii-Avacha Volcanic Cluster as inferred from observations of local seismicity and from the regime of adjacent thermal springs // Journal of Volcanology and Seismology. 2017. T. 11. B. 5. C. 321-334. DOI: 10.1134/S0742046317050049.

McClure, M.W.: CFRAC (version 1.2) Complex Fracturing Research Code User's Guide (version 20), December, (2014).

McClure, M.W., and Horne, R.N.: *Discrete Fracture Network Modeling of Hydraulic Stimulation: Coupling Flow and Geomechanics*, Springer, (2013), doi:10.1007/978-3-319-00383-2.

Sigmundsson, F., Hooper, A., Hreinsdorttir, S., et al., Segmented lateral dyke growth in a rifting event at Barrparbunga volcanic system, Iceland, *Nature,* 2015, vol. 517, pp. 191–194. doi 10.1038/nature14.

Zoback M.D.: Reservoir Geomechanics, Cambridge University Press, (2007), 448 p.